Journal of Radioanalytical and Nuclear Chemistry (2021) 329:337–349
https://doi.org/10.1007/s10967-021-07761-5

Diethylenetriamine functionalized silica gel for adsorption of uranium from aqueous solution and seawater

P. Amesh[1,2] · K. A. Venkatesan[1,2] · A. S. Suneesh[3] · Deepak K. Gupta[4] · T. R. Ravindran[4]

Received: 18 February 2021 / Accepted: 27 April 2021 / Published online: 2 June 2021

Abstract

The diethylenetriamine (DETA) organic moiety was anchored covalently on the surface of silica gel to obtain a surface-modified adsorbent abbreviated as Si-DETA. The adsorbent was characterized by FT-IR, Raman spectroscopy, thermogravimetry, scanning electron microscopy, and energy dispersive X-ray analysis. The adsorption behavior of uranium on Si-DETA was studied as a function of pH of the aqueous phase, duration of contact time, and concentration of uranium in the aqueous phase. The kinetics of uranium adsorption on Si-DETA was fitted with pseudo-first order and pseudo-second order kinetic models. The adsorption isotherm obtained from uranium loading was fitted into popular models such as Langmuir, Freundlich, Temkin, and D-R adsorption isotherms. The statistics of fitting revealed that the Langmuir adsorption model obeyed the adsorption data. The performance of the adsorbent was also evaluated under dynamic conditions by passing feed solution containing uranium in a buffered solution and seawater into a fixed bed column containing Si-DETA. The results were compared with those obtained in a batch mode. The study showed the possibility of using Si-DETA for the separation and recovery of uranium from aqueous waste and seawater.

Keywords Adsorption · Silica gel · Diethylenetriamine · Uranium · Seawater

Introduction

Nuclear reactors are the promising option for clean energy production compared to coal, bio-fuels, and other natural gas products [1–5]. Nuclear reactors are supplementing about 10% of the global power requirement at present [4–8]. In all cases, uranium has been chosen as the primary fuel for operating nuclear reactors. According to the International Atomic Energy Agency (IAEA), at least 65 thousand tons of uranium per year are required to produce 10% electricity [4–8]. The primary resource of uranium employed for the fabrication of fuel is from the land-based ores, essentially obtained by mining [8–10]. Due to the enormous consumption of uranium, its availability from the earth's crust is likely to be exhausted in the near future [9–11]. In view of these, there is a need to look for an alternative resource of uranium for the sustained production of nuclear power. One such resource is seawater, which is considered the best resource for uranium owing to the large quantity of uranium present in seawater (4.5 trillion kilograms) [11–14]. However, the difficulty associated with the separation of uranium from seawater is the ultra-trace concentration of uranium in seawater (3.3 ppb) and coexistence of several other ions, which interfere during the separation of uranium. In spite of this, the attractive feature of seawater is the total quantity of uranium present in the ocean ($\sim 4.5 \times 10^{12}$ kg), which is drawing the attention of energy-policy makers and researchers to develop methods and materials for the recovery of uranium from seawater. In addition, the mining of uranium from terrestrial sources also generates aqueous waste containing a significant amount of uranium. The presence of uranium in these wastes contaminates the groundwater raising contamination levels beyond the permissible level of tolerable

✉ K. A. Venkatesan
kavenkat@igcar.gov.in

1 Reprocessing Research and Development Group, Indira Gandhi Centre for Atomic Research, Kalpakkam 603 102, India

2 Homi Bhabha National Institute, Anushaktinagar, Mumbai, Maharashtra 400094, India

3 Materials Chemistry and Metal Fuel Cycle Group, Indira Gandhi Centre for Atomic Research, Kalpakkam 603 102, India

4 Materials Science Group, Indira Gandhi Centre for Atomic Research, Kalpakkam 603 102, India

daily intake (TDI) limit of 15 µg L^{-1} (by WHO) [15]. This kind of contamination also calls for the separation of trace levels of uranium from wastewater.

The major challenges in the separation and recovery of uranium from waste water arising from mines and seawater are the trace level concentration of uranium coexisting with high amounts of other interfering ions [16–19]. These challenges eliminate the conventional separation techniques such as solvent extraction and calls for the development of advanced methods and materials for the separation of uranium from aqueous wastes and seawater. On the other hand, the solid phase adsorption technique is a proven and viable method for separating trace level concentration of metal ions present in a large volume of the aqueous phase containing significant amount of other interferences. To further improve the selectivity of solid adsorbents towards target metal ions, the surface of the solid phase is usually modified with target specific organic functional groups. In fact, such organo functionalized adsorbent materials are indeed suitable for the separation of uranium from aqueous waste, mine wastes and seawater [20–23].

In this perspective, several authors reported organo functionalized solid-phase adsorbents for separation of uranium from an aqueous solution. For instance, Dominic et al. prepared silica particles modified with Schiff base for the extraction of uranium from acidic solution and reported the uranium extraction capacity of 95 mg g^{-1} from pH 6 solution [23]. Ali et al. designed Rhodamine-B modified silica for the adsorption of uranium from aqueous waste [24]. The results showed that more than 94% of uranium was adsorbed from waste solution containing 168 mg L^{-1} of uranium at pH 5. Anbeer et al. [25] synthesized silica gel modified with tris(2-aminoethyl)amine moiety. The author reported about 98% of uranium adsorption from uranium contaminated water containing 1 mg L^{-1} at pH 7. Similarly, Liu et al. [26] synthesized amine-functionalized magnetic mesoporous silica (SBA-15) for uranium adsorption and reported the apparent adsorption capacity of 395.05 mg g^{-1} from pH 6 solution.

We previously reported amidic succinic acid anchored silica gel for the adsorption of uranium and reported the uranium adsorption capacity of 61 mg g^{-1} from the aqueous phase and 16 mg g^{-1} from synthetic seawater [27]. However, the same amidic succinic acid anchored on mesoporous silica, improved the uranium adsorption capacity to 850 mg g^{-1} [28]. We also reported diethylenetriamine functionalized iron oxide with the uranium adsorption capacity of ~ 230 mg g^{-1} from pH 6 solution [29], and diethylenetriamine functionalized mesoporous silica with the adsorption capacity of ~ 1000 mg g^{-1} for uranium [30]. In this present study, the silica gel was chosen as a base solid matrix in contrast to the above mentioned high capacity adsorbents due to the convenient of particle size (100–150 µm) for facile column operation (Lower particle size are not suitable due to chocking during column study). In this paper, the results on the preparation of the diethylenetriamine anchored silica gel (Si-DETA) and studies on the adsorption behavior of uranium (U(VI)) from aqueous solution on Si-DETA have been reported. The influence of pH, time, and initial concentration of uranium in the feed solution on the adsorption behavior of uranium was studied in batch equilibration mode. The adsorption performance of Si-DETA was also evaluated under dynamic column conditions. The adsorbent Si-DETA was also tested for the adsorption of uranium from seawater spiked with natural uranium under dynamic column conditions and compared the results with those obtained in batch and column studies.

Experimental

Materials

HPLC or AR grade chemicals were used for all experimental studies. Silica gel (Aldrich, > 99% purity, ~ 100 µm average particle size) was employed for anchoring of organic moiety. The precursor materials employed for anchoring were (3-chloropropyl)trimethoxysilane (Aldrich, 99.5%), diethylenetriamine (E-Merck, AR grade, 97%). Toluene (Aldrich, HPLC grade) and chloroform (Aldrich, HPLC grade) were used as solvents. Acetic acid (Rankem, AR grade) and sodium acetate (SD fine, purity > 99%) were used for the preparation of buffer solution. Nitric acid (Rankem, AR grade) was employed for pH adjustment. The uranyl nitrate hexahydrate was obtained from Nuclear Fuel Complex, Hyderabad, India. A concentrated stock solution of uranium was prepared by dissolving the required quantity of uranyl nitrate in a nitric acid medium (50 mg mL^{-1} uranium in 0.1 M HNO_3).

Instrumentation

The scanning electron micrographic (SEM) image of silica gel, Si-DETA, and uranium loaded Si-DETA were recorded using Field Emission Gun-Scanning Electron Microscopy (Carl-ZEISS, Germany). The elemental composition of the scanned image was obtained using an Energy-dispersive X-ray spectroscopy analyzer (Oxford EDX analyzer, UK) working in tandem with the SEM unit. The FT-IR spectrum of silica gel, Si-DETA, and uranium loaded Si-DETA was recorded using an FT-IR spectrometer (Tensor II, Bruker, Germany). For recording FT-IR spectra, KBr powder (dry) was mixed with the sample (1% weight) and ground using pestle and motor. The powder was then made into a disk of a thickness of ~ 0.1 mm and a diameter of ~ 10 mm. The transmittance spectrum of the disk was recorded using an FT-IR spectrometer. The Raman spectra of silica gel, Si-DETA, and

uranium loaded Si-DETA were recorded by Renishaw PLC Raman microscope system (Gloucestershire, UK) equipped with a Leica microscope using 785 nm excitation laser (300 mW). The thermal analysis of the solid sample was performed in a thermogravimetric analyzer (TGA/SDTA 851e, Metler Tolledo, UK). The concentration of uranium present in the aqueous phase was determined by a spectrophotometric method (UV-2100, Shimadzu, Japan) using Arsenazo III as a coloring agent.

Synthetic procedure for preparation of Si-DETA

Preparation of intermediate compound

The Si-DETA was prepared by the two-step reaction. The first step involves the reaction between (3-chloropropyl) trimethoxysilane (27.4 mmol, 5 mL) and diethylenetriamine (27.6 mmol, 3 mL) (1:1 mol ratio) to obtain the intermediates. The entire reaction was carried out in a chloroform medium for 6 h at 298 K. The intermediates formed are abbreviated as ATDTS and ADTS, as shown in Fig. 1.

Surface modification of silica gel with diethylentriamine

The intermediate compounds (amount varied) obtained in the above reaction was then allowed to react with silica gel (1 g) (pre-heated at 333 K in the air for about an hour) in a toluene medium at 350 K for about 12 h. The amount of intermediate required for efficient functionalization on to silica gel was optimized by determining the uranium distribution coefficient on the obtained product from pH 3 and 6 solutions. The distribution coefficient was measured as discussed below. The optimum ratio of intermediate to silica gel was determined from the distribution coefficient measurements, and the same was employed for the bulk preparation of Si-DETA.

Adsorption of uranium from aqueous solution

The batch equilibration method was employed for testing the adsorption behavior of uranium from aqueous solutions at 298 K. For this experiment, about 50 mg of the adsorbent (Si-DETA) was equilibrated with 10 mL of uranyl nitrate solution ($U = 200$ mg L^{-1}) taken in a stoppered glass tube. The pH of the aqueous phase, pH 1 and 2, was adjusted using diluted nitric acid, whereas the pH 3 and above was made with sodium acetate-acetic acid (both 0.2 M) buffer solution. The acetate buffer was employed for adjusting the pH of the solution from 3 and above to prevent the hydrolysis of uranyl ion in the aqueous solution. It should be noted that extensive hydrolysis leads to the precipitation of uranyl ions from the solution as hydroxides. However, it was found that the acetate-acetic acid buffer solution prevents the precipitation of uranium, which was confirmed by the material balance of uranium during the experimental study [31, 32]. The stoppered glass tubes were then equilibrated by rotating them in an upside-down manner for 6 h, at the speed of 50–60 revolutions per minute (rpm). After equilibration, an aliquot was taken from the aqueous phase. The concentration of uranium present in the aqueous phase was determined by a spectrophotometric method using Arsenazo III as a chromophore, described elsewhere [33]. The distribution coefficient of uranium (K_d, mL g^{-1}) on Si-DETA was determined using Eq. 1.

$$K_d \text{ of U(VI)} = \frac{[U]_i - [U]_f}{[U]_f}\left(\frac{V}{m}\right) \text{mL g}^{-1} \quad (1)$$

where $[U]_i$ and $[U]_f$ represent the concentrations of U(VI) in the aqueous phase before and after equilibration, respectively, and V (in mL) and m (in g) are the volumes of the aqueous phase and weight of Si-DETA taken for equilibration. All the adsorption experiments were performed in triplicate, and the distribution coefficient of U(VI) obtained in the triplicate agreed well with each other, with less than a 5% difference.

Kinetics of uranium adsorption

The time dependency of uranium adsorption on Si-DETA was studied using batch equilibration mode at two different uranium concentrations (200 and 500 mg L^{-1}) present in pH 3 and 6 buffer solutions at 298 K. The procedure adopted for the batch equilibration is similar to that discussed above. However, at various intervals of time, the equilibration was stopped, and an aliquot was taken from the aqueous phase for determining uranium concentration. The amount of uranium adsorbed on Si-DETA at a particular time (q_t, in mg g^{-1}) was determined using Eq. 2. A similar batch experiment was adopted for the next time interval.

$$q_t = [U]_i - [U]_f\left(\frac{V}{m}\right) \text{mg g}^{-1} \quad (2)$$

Column studies

The uranium adsorption behavior on Si-DETA was studied under dynamic conditions by column method. In this study, about 1 g of Si-DETA was soaked in Millipore water for 30 min prior to the packing in a glass column of diameter 8 mm. The packed column was pre-conditioned with 50 mL of pH 6 buffer solutions (acetic acid and sodium acetate). A feed solution composed of uranyl nitrate ($U = 200$ mg L^{-1}) in pH 6 buffer was passed into the column at a particular flow rate (1 mL per minute). The effluent that emerged out from the column was collected in 10 mL standard flasks

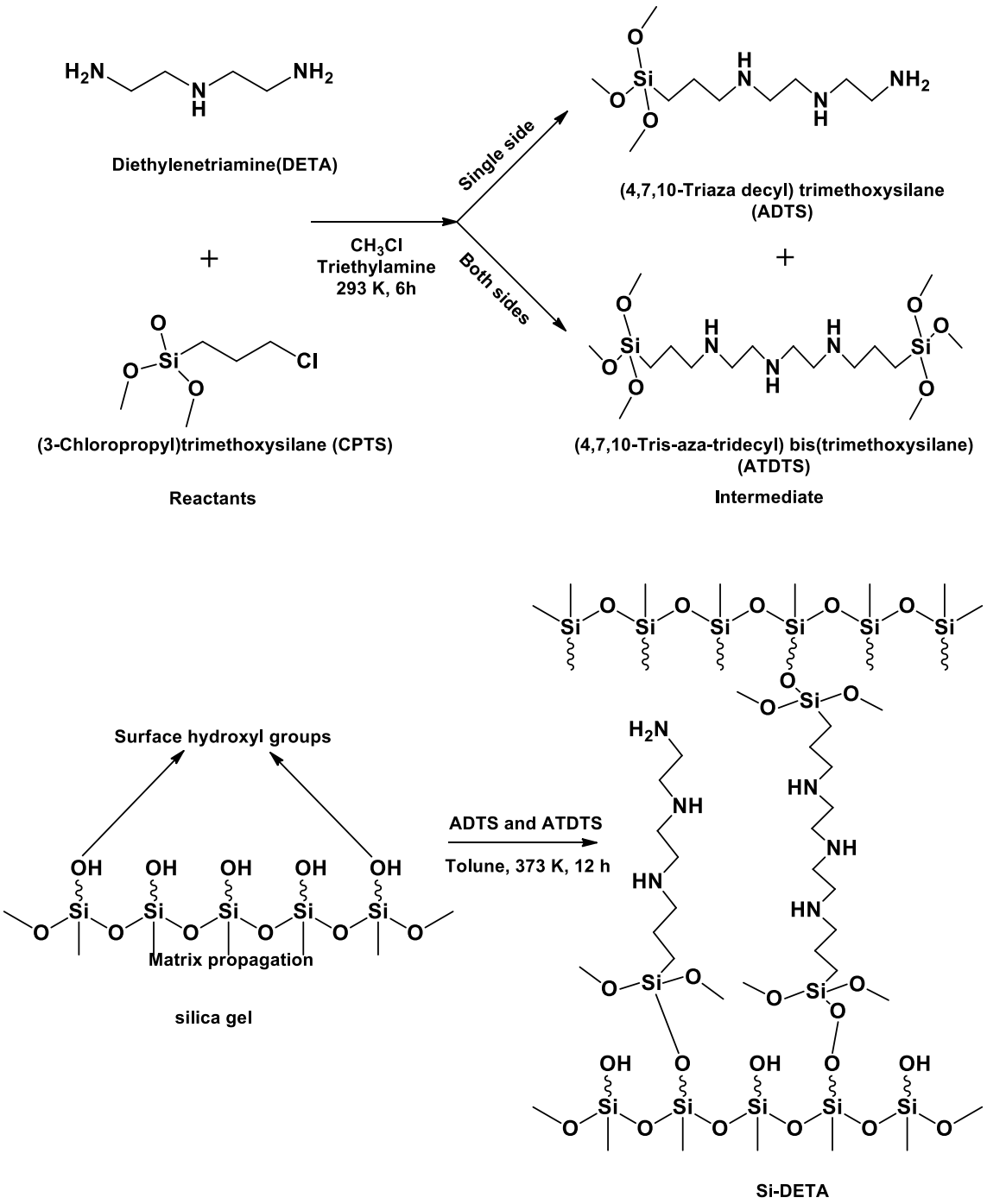

Fig. 1 Reaction scheme for the synthesis of Si-DETA

sequentially. The concentration of uranium present in the flask was determined by the spectrophotometric method discussed above. The effluent was collected until the concentration of uranium in the effluent (C_t) nearly becomes equal to the uranium concentration in the feed (C_0). A similar procedure was also adopted for the feed solution passed at a flow rate of 0.5 mL min^{-1}, and other conditions remaining the same.

The Si-DETA was also tested for the adsorption of uranium from seawater spiked with uranium in dynamic mode. A feed solution of seawater collected from the coastal area of Kalpakkam, India, was spiked with natural uranium with a concentration of 100 mg L^{-1} and passed into the column. The effluent was collected in a 10 mL standard flask, as indicated above, and the concentration of uranium was determined, as stated above. For all these dynamic mode

experiments, various break-through curves were obtained by plotting the ratio of uranium concentration in the effluent to feed versus the time of feed solution passed.

Effect of possible interfering ions during adsorption of uranium on Si-DETA

It is vital to know the adsorption behavior of uranium from aqueous solutions containing possible interfering ions such as CO_3^{2-}, Na^{+}, Cr^{+3}, Fe^{+2}, Fe^{+3}, Co^{+3}, Ni^{+3} and VO^{2+}. In order to know the adsorption behavior of uranium in the presence of these interfering ions, the batch experiment was performed by equilibrating ~ 50 mg of Si-DETA with 10 mL of the aqueous solution containing 200 mg L^{-1} of uranium and 500 mg L^{-1} of each interfering ion. Batch experiments were performed for each interfering ion separately. After equilibration, an aliquot was taken from the aqueous phase, and the uranium concentration was determined, as discussed above.

Recycling studies

The adsorbent can be regarded as valuable only when it is possible to recycle the adsorbent as many times as possible. To determine the number of reusable cycles, a batch experiment was performed for loading of uranium on Si-DETA to its maximum capacity, followed by stripping with 0.1 M HNO_3. For this experiment, 0.5 g of adsorbent was equilibrated with 10 mL of the aqueous solution containing 1000 mg L^{-1} of uranium at pH 6 for 6 h, as discussed above. After equilibration, the aqueous phase was separated by centrifugation, and the adsorbent was treated with 10 mL of 0.1 M of HNO_3 (three times) to strip back the uranium. The aqueous strip solution was collected together and the concentration of uranium was determined by a spectrophotometric method, as discussed above. This process is repeated about 10 times with the same adsorbent.

Results and discussion

Optimization of functional groups on Si-DETA

Si-DETA was prepared by a two-step chemical reaction. The first step involved the reaction between DETA and CPTS to obtain the intermediates ATDTS and ADTS as shown in Fig. 1. This was further reacted with silica gel to obtain Si-DETA. To optimize the amount of intermediate required for effective functionalization of silica gel, the weight ratio of the intermediate to silica gel taken in the second step of the reaction shown in Fig. 1 was varied, and the product obtained was tested for the adsorption of uranium at pH 3 and 6. Figure 2 shows the variation of the distribution coefficient of uranium on Si-DETA obtained at different weight ratios of intermediate to silica gel. It can be seen that the distribution coefficient of uranium on Si-DETA increases with increasing the weight ratio of intermediate to silica gel and reached a saturation value at the intermediate to silica gel weight ratio of 5:1. Based on these studies, the optimum amount of intermediate compound to silica gel was fixed at 5:1 for the preparation of bulk quantity of Si-DETA.

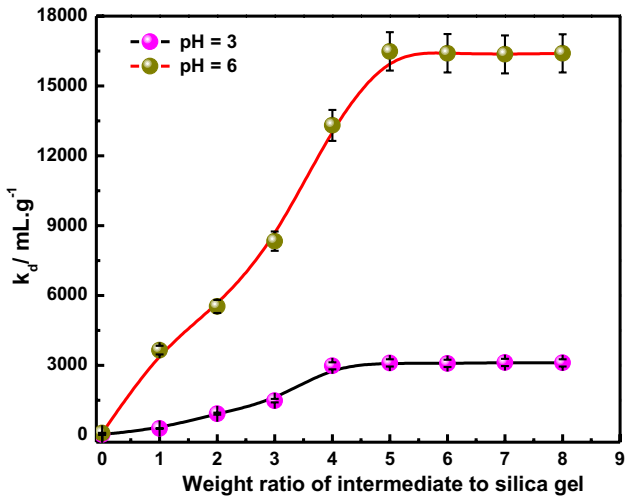

Fig. 2 Optimization of functional groups on Si-DETA. Variation in the distribution coefficient of U(VI) on Si-DETA at pH 3 and 6 studied as a function of weight ratio of intermediate to silica gel. Adsorbent: 50 mg of Si-DETA prepared at different weight ratios of intermediate to silica gel. Aqueous phase: Uranyl nitrate solution (U = 200 mgL^{-1}) at pH 3 and pH 6. Temperature: 298 K

Characterization of adsorbent

FT-IR and Raman spectroscopy

The FT-IR spectra of Si-DETA and uranium loaded Si-DETA (abbreviated as Si-DETA-U) are shown in Fig. 3. The FT-IR spectra of Si-DETA show the transmittance bands corresponding to the N–H stretching at 3476 cm^{-1} and N–H bending vibrations at 1457 and 1384 cm^{-1} [24–26, 29, 30]. The hydroxyl group stretching and bending vibrational modes are observed at 3475 and 1644 cm^{-1} due to the presence of adsorbed water molecules on the surface of Si-DETA. The bands at 1075 and 786 cm^{-1} are due to the vibrations arising from the silica matrix [24–26, 29, 30]. All these vibrational bands confirm the presence of amine moiety on silica gel.

The Raman spectra of silica gel and Si-DETA are shown in Fig. 4. The Raman spectrum of silica gel shows several bands at 1232, 1318, and 1695, etc. All these vibrational bands are due to the Si–O stretching, Si–O–Si stretching, Si–O–Si bending, and other miscellaneous silica matrix

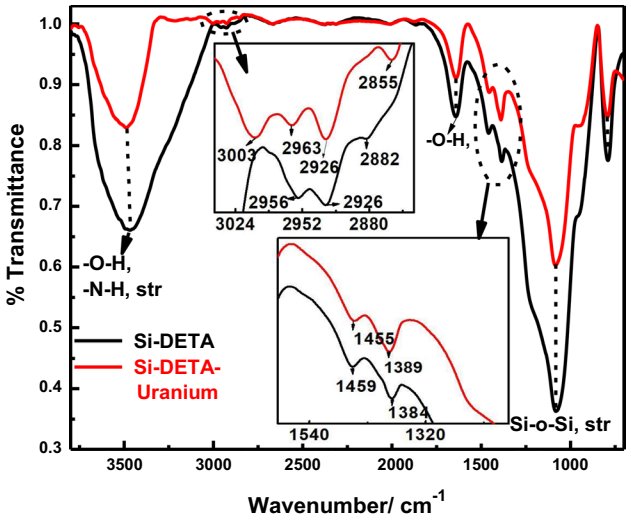

Fig. 3 Comparison in the FT-IR spectrum of Si-DETA and U(VI) loaded Si-DETA

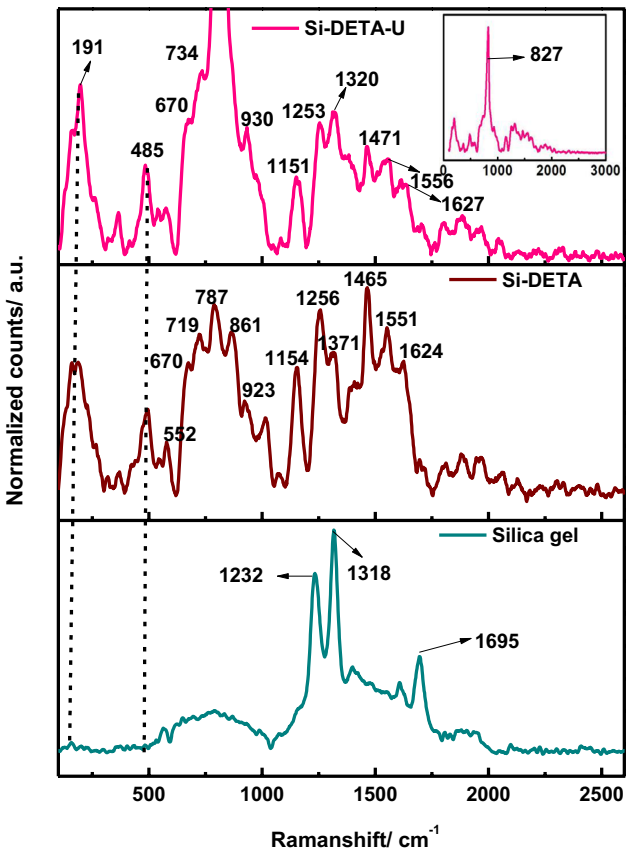

Fig. 4 Comparison in Raman spectrum of silica gel (bottom), Si-DETA (middle) and uranium adsorbed Si-DETA (top)

vibrations [29, 30]. The Raman spectra of Si-DETA showed various amine bands in the range of 1150–1630 cm^{-1}. The skeletal C–C stretchings are observed in the range of 670–1060 cm^{-1}, C–N bands in the range of 1030–1080 cm^{-1}. The Raman spectrum of Si-DETA also confirms the presence of amine moiety on silica gel [29, 30, 34, 35].

Thermogravimetry

The amount of organics present on Si-DETA was quantified by thermogravimetric analysis. Figure 5 shows the thermogravimetric analysis of silica gel and Si-DETA. The curve obtained for silica gel shows a 7% weight loss in the temperature range 311–430 K, which is due to the loss of water molecules adsorbed on the surface of silica gel. Beyond 430 K and up to 1200 K, the weight loss is about 3%, which could be due to the cross condensation of hydroxyl groups present on the surface of silica gel leading to the loss of water molecules. In the case of Si-DETA, about 12% water loss occurs in the temperature range 311–430 K due to the loss of adsorbed water molecules. In addition, there is also a two-step weight loss occurring in the temperature range 430–1000 K, which is due to the decomposition of organic moiety present on the surface of Si-DETA. The weight loss due to the decomposition of organics was determined to be about 15%, which corresponds to the presence of 0.56 mmol of an organic moiety (DETA) per gram of Si-DETA.

Effect of pH on the adsorption of uranium

Figure 6 shows the pH (equilibrium) dependency of uranium adsorption on Si-DETA. It can be seen that that the distribution coefficient of U(VI) on Si-DETA is low in the lower pH range ($K_d < 500$ at pH ≤ 2), and the distribution coefficient increases with an increase in the pH of the aqueous phase

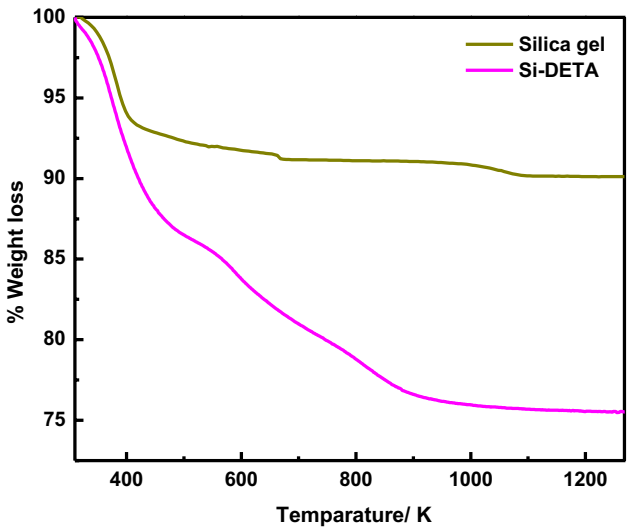

Fig. 5 Thermogravimetric pattern obtained for silica gel and Si-DETA

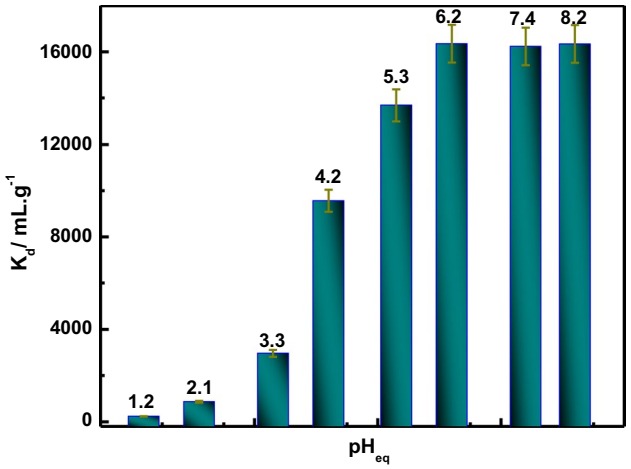

Fig. 6 Variation in the distribution coefficient of uranium on Si-DETA as a function of equilibrium pH. Adsorbent: 50 mg of Si-DETA. Aqueous phase: Uranyl nitrate solution ($U = 200$ mgL^{-1}) at pH 1–8. Temperature: 298 K

followed by saturation in K_d values at pH greater than 6. This trend can be explained by considering the protonation of amine groups on Si-DETA by H^+ ions at lower pH values. Since amine groups are responsible for the adsorption of uranium on Si-DETA, the protonation of amine lowers the availability of amine moiety for coordination with uranium. However at higher pH, the protonation of amine is less and the Kd of U(VI) increases with increase in the pH of aqueous phase. Since the K_d of U(VI) was maximum at pH 6 (~ 17,000 mL g^{-1}) and beyond, further adsorption studies were carried out at pH 6.

Kinetics of uranium adsorption

The variation in the adsorption (q_t/mg g^{-1}) of uranium on Si-DETA as function of time is shown in Fig. 7. The experiment was carried out at pH 3 and 6 and at the uranium concentrations of 200 mg L^{-1} and 500 mg L^{-1} in aqueous phase. It can be seen that the adsorption of uranium increases with increase in the duration of equilibration and reaches saturation beyond 120 min. The adsorption is rapid in the initial stages of equilibration at both the concentrations and pH values. The adsorption of uranium at pH 6 is more than that observed at pH 3 at all time intervals. Therefore, all batch experiments were conducted for 600 min to ensure the establishment of equilibrium. The kinetic data obtained at pH 3 and 6 were modeled with pseudo-first order and pseudo-second order rate equations shown in Eqs. 3 and 4, respectively [36–38]. The fitting parameters and the rate constants are tabulated in Table 1. From the fitting parameters, it is apparent that the adsorption kinetics is described well by pseudo-second order kinetics.

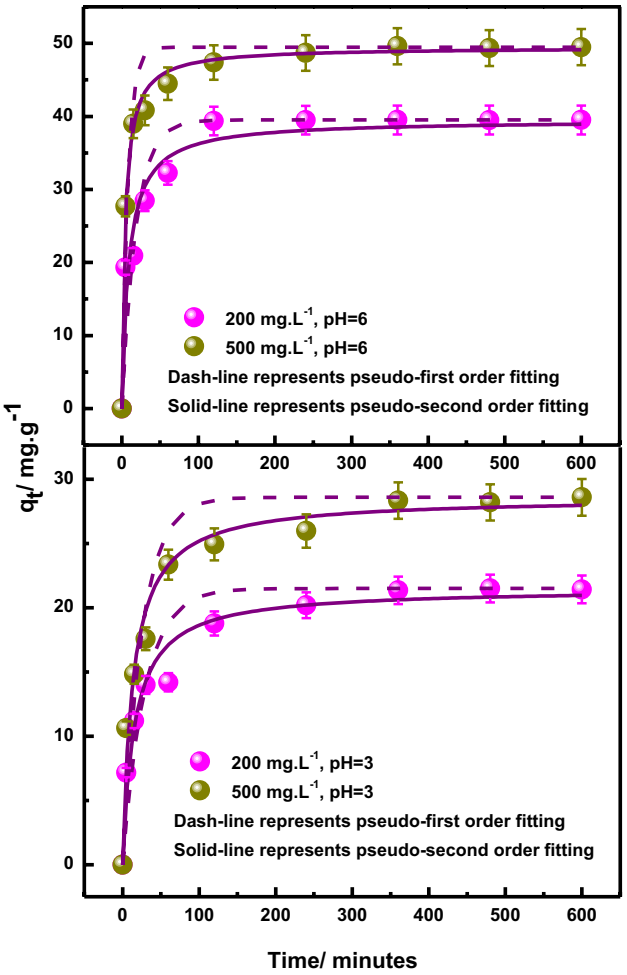

Fig. 7 Variation in the amount of uranium loaded on Si-DETA as a function of various intervals of time. Adsorbent: 50 mg of Si-DETA. Aqueous phase: Uranyl nitrate solution (200 and 500 mg L^{-1}) at pH 3 and pH 6. Temperature: 298 K

$$q_t = q_e\left(1 - e^{-k_1 t}\right) \tag{3}$$

$$q_t = \frac{k_2 q_e^2 t}{1 + k_2 q_e t} \tag{4}$$

where q_t (mg g^{-1}) is the amount of U(VI) adsorbed on Si-DETA at different intervals of time, q_e is the amount of U(VI) adsorbed at equilibrium, k_1 (min^{-1}) and k_2 (g mg^{-1} min^{-1}) are the pseudo-first order and pseudo-second order rate constants, respectively.

The adsorption isotherm

The effect of uranium concentration in aqueous phase on the adsorption of uranium (VI) on Si-DETA was investigated at pH 3 and 6. Figure 8 shows the adsorption

Table 1 The non-linear regression analysis of the kinetics of uranium adsorption on Si-DETA and the resultant fitting parameters. Aqueous phase: 10 mL of aqueous solution containing 200 mg L^{-1} or 500 mg L^{-1} U(VI) in pH 3 and pH 6 solution. Adsorbent phase: 50 mg of Si-DETA

Equilibrium pH of aqueous phase	Kinetic model	Parameter	Amount of uranium in aqueous phase	
			200 mg L^{-1}	500 mg L^{-1}
3	Pseudo first order	R^2	0.865	0.918
		χ^2	5.4	7.2
		k_1/min^{-1}	3.4×10^{-2}	3.9×10^{-2}
	Pseudo second order	R^2	0.970	0.980
		χ^2	1.5	1.8
		k_2/mg g^{-1} min^{-1}	3.0×10^{-3}	2.6×10^{-3}
6	Pseudo first order	R^2	0.908	0.946
		χ^2	15.8	12.9
		k_1/min^{-1}	5.3×10^{-2}	1.2×10^{-2}
	Pseudo second order	R^2	0.961	0.994
		χ^2	6.6	1.2
		k_2/mg g^{-1} min^{-1}	2.8×10^{-3}	4.7×10^{-3}

of uranium (VI) (q_e/mg g^{-1}) on Si-DETA studied as a function of equilibrium concentration of uranium in aqueous phase. The loading of uranium on Si-DETA increases with the increase in the equilibrium concentration of uranium in aqueous phase, reaches the saturation at higher concentration levels. The loading of uranium at pH 6 is more than that observed at pH 3. The experimental isotherms were fitted into popular models such as Langmuir, Freundlich, Temkin, and Dubinin–Radushkevich (D–R) adsorption models represented in Eqs. 5–8 respectively [39–42]. The model parameters and statistical fitting parameters are shown in Table 2. From the statistics of fitting, it is apparent that the Langmuir adsorption model fits the experimental data well as compared to other models.

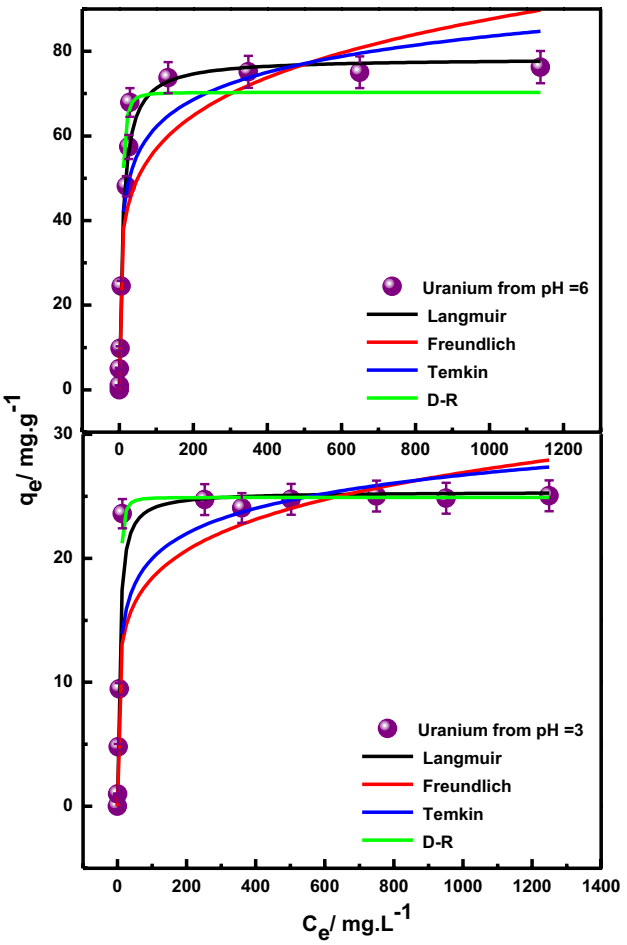

Fig. 8 Variation in the loading behaviour of uranium on Si-DETA as a function of equilibrium concentration of uranium in aqueous phase. Adsorbent: 50 mg of Si-DETA. Aqueous phase: Uranyl nitrate solution ($U = 10$–2000 mg L^{-1}) at pH 3 and pH 6. Temperature: 298 K

$$q_e = \frac{K_L Q_o C_e}{1 + K_L C_e} \tag{5}$$

$$q_e = K_F C_e^{1/n} \tag{6}$$

$$q_e = \frac{RT}{b_T} \ln A_T C_e \tag{7}$$

$$q_e = q_m e^{-\beta\varepsilon^2} \tag{8}$$

where Q_o is the apparent Langmuir adsorption capacity (mg g^{-1}), K_L is the Langmuir adsorption constant (mg L^{-1}), C_e is the equilibrium amount of U(VI) in the aqueous phase (mg L^{-1}), q_e is the amount of U(VI) in Si-DETA at equilibrium (mg g^{-1}), $\frac{1}{n}$ is the heterogeneity parameter and K_F is the Freundlich adsorption constant of the adsorbent, β is Dubinin–Radushkevich constant (mol^2 J^{-1}), q_m is the D–R apparent capacity (mg/g), ε is the Polanyi potential and A_T and b_T are the constants. From Langmuir fitting, the apparent

Table 2 Fitting parameters obtained by modelling of uranium adsorption on Si-DETA. Aqueous phase: 10–2000 mg L^{-1} in pH 3 and 6 solution. Adsorbent: 50 mg of Si-DETA

Model	Parameter	pH 3	pH 6
Langmuir	Q_o/mg g^{-1}	25.36	78.3
	K_L/mg L^{-1}	1.75×10^{-2}	1.01×10^{-2}
	R^2	0.957	0.986
	χ^2	4.9	13.9
Freundlich	$1/n$	0.165	0.187
	K_F/mg g^{-1}	8.6	24.0
	R^2	0.815	0.814
	χ^2	21.3	193.4
Temkin	b_T/J mol^{-1}	845.8	266.71
	A_T/L g^{-1}	9.13	8.04
	R^2	0.883	0.900
	χ^2	13.5	103.29
D–R	q_m/mg g^{-1}	24.90	70.2
	β/mol^2 J^{-1}	-4.5×10^{-6}	-6.8×10^{-6}
	$E_{D-R}=\frac{1}{\sqrt{-2\beta}}$/J mol^{-1}	1.1×10^{-4}	7.3×10^{-5}
	$\varepsilon = RT\ln\left(1+\frac{1}{C_e}\right)$/ mol^2 J^{-1}	1.77	1.95
	R^2	0.975	0.948
	χ^2	2.8	53.8

Langmuir adsorption capacity of uranium on Si-DETA at pH 6 was determined to be 78 mg g^{-1}.

The binding of uranium on Si-DETA was also confirmed by FT-IR and Raman spectroscopy. The FT-IR spectrum of uranium loaded Si-DETA sample is shown in Fig. 3 and compared with Si-DETA before uranium loading. It can be seen that the amine group N–H bending vibrations is shifted from 1384 to 1389 cm^{-1}. This could be due to the coordination of uranyl ions with amine moieties. The asymmetric stretching mode of uranyl ion around 900 cm^{-1} was not observed in the FT-IR spectrum [43, 44], perhaps due to the masking of intense Si–O stretching vibrations. The Raman spectra of uranium adsorbed Si-DETA showed all the peaks corresponding to C–C, C–N, C–H, and N–H, bands similar to Si-DETA. However, the various N–H vibrational modes in the region 1465, 1551, 1624 cm^{-1} in Si-DETA are shifted to 1471, 1556, 1627 cm^{-1}, which could be due to the coordination of uranyl ion with amine moieties [43, 44]. The Raman bands at 734, 827 cm^{-1} are due to the stretching vibrations of coordinated uranyl ions [43–45]. All these observations confirmed the adsorption of uranyl ions on Si-DETA occurs through the coordination of amine functional groups present on Si-DETA.

Figure 9 shows the SEM image of Si-DETA, and uranium loaded Si-DETA. It can be seen that both the adsorbents have appeared as particles having a size of ~ 100 µm with irregular shape. The surface morphology of the adsorbent was not affected upon anchoring of amine moieties on Si-DETA, and also after uranium adsorption. The EDX spectra of adsorbents are also shown in Fig. 9. The Si-DETA shows the elements such as carbon and nitrogen in addition to silicon and oxygen, indicating the presence of functional groups on silica gel. The uranium loaded Si-DETA shows the presence of adsorbed uranium on silica gel.

Column studies and analysis of the break-through curve

Figure 10 shows the breakthrough curve obtained for the adsorption of uranium from an aqueous solution containing uranium (200 mg L^{-1}) at pH 6. The breakthrough curve was obtained by plotting the ratio of the concentration of uranium in the effluent (C_t) to feed (C_0) as a function of time. The ratio of C_t/C_0 is known as the breakthrough. The column study was carried out at two different flow rates (1 mL min^{-1} and 0.5 mL min^{-1}). It can be seen that the onset of breakthrough occurs after passing about 200 mL of feed solution at the flow rate of 1 mL min^{-1}, whereas the onset of breakthrough occurs after passing 300 mL of the feed solution at a flow rate of 0.5 mL min^{-1}. The uranium adsorption capacity at the onset of breakthrough was determined to be 40 mg g^{-1} and 60 mg g^{-1} at flow rates of 1 mL min^{-1} and 0.5 mL min^{-1}. For a better understanding of the complete breakthrough curve up to $C_t/C_0 \sim 1$, the experimental data were fitted into the Thomas model of the form shown in Eq. 9 [46, 47], and the fittings are also shown in Fig. 10.

$$\frac{C_t}{C_o} = \frac{1}{1+\exp\left(\frac{mq_oK_{Th}}{Q} - \frac{C_oK_{Th}t}{1000}\right)} \quad (9)$$

where m is the mass of dry Si-DETA taken in a column packing, K_{Th} is the Thomas rate constant for the adsorption of U(VI) in a fixed bed column, Q is the volumetric flow rate (L min^{-1}), C_o the concentration of uranium (mg L^{-1}) in the feed and C_t is the concentration of uranium in the effluent.

The Thomas model is generally employed to describe the behavior of metal ion/adsorbent's adsorption in a fixed bed column in a continuous mass flowing system. The Thomas model assumes pseudo-second order adsorption kinetics and Langmuir model with no axial dispersion of mass during the continuous flow of feed into the column [48, 49]. Since the adsorbent in the present study follows pseudo-second order kinetics and Langmuir type of adsorption, the column breakthrough behavior was fitted using the Thomas model. The fittings are shown in Fig. 10. The fitting parameters, such as Thomas rate constant and other statistic parameters obtained from fitting of the experimental data are tabulated in Table 3. From the Thomas model fitting, the uranium adsorption capacity at 100% breakthrough was determined

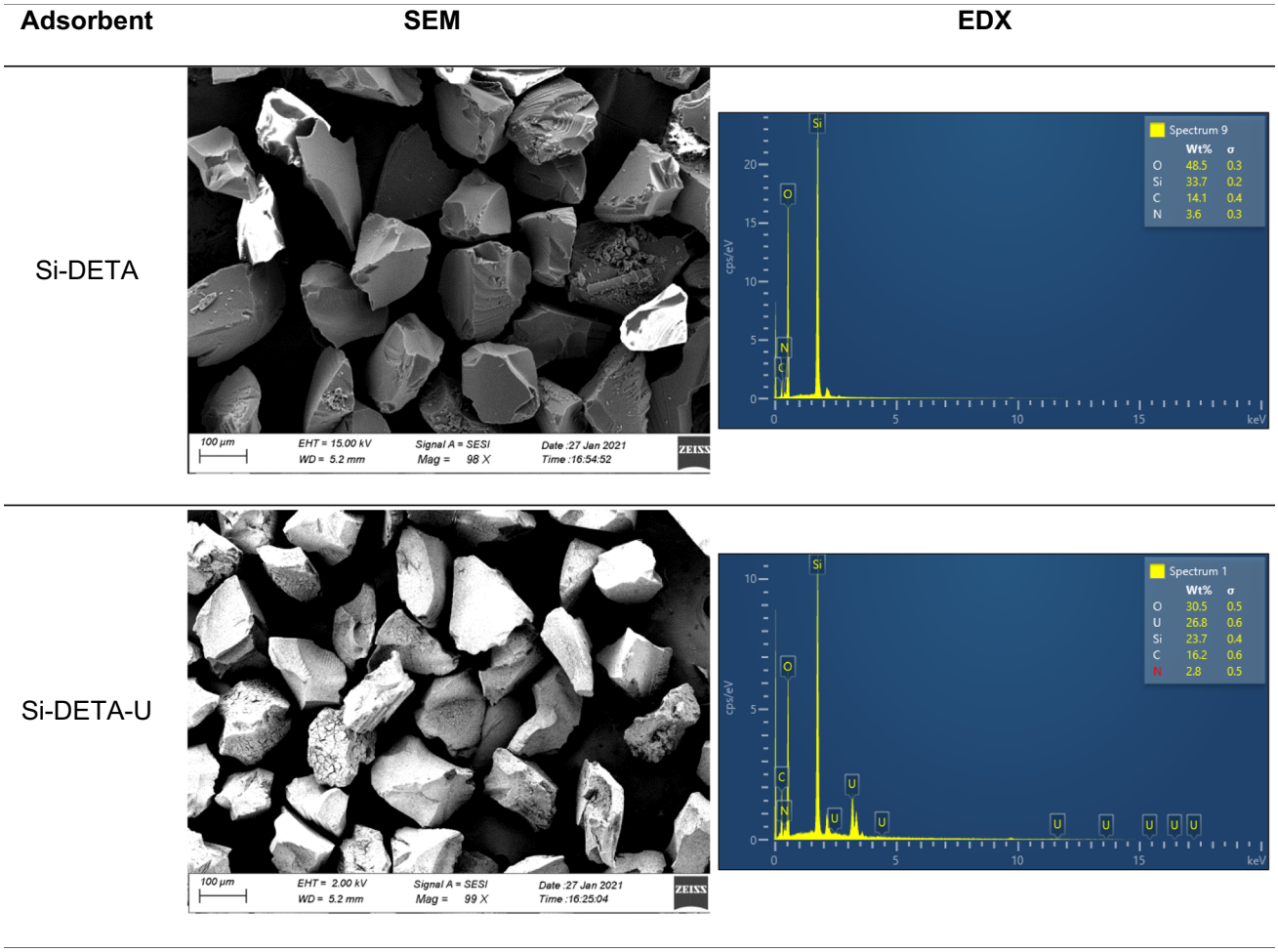

Fig. 9 Scanning electron microscopic images of Si-DETA and Si-DETA-U and energy dispersive X-ray spectroscopy

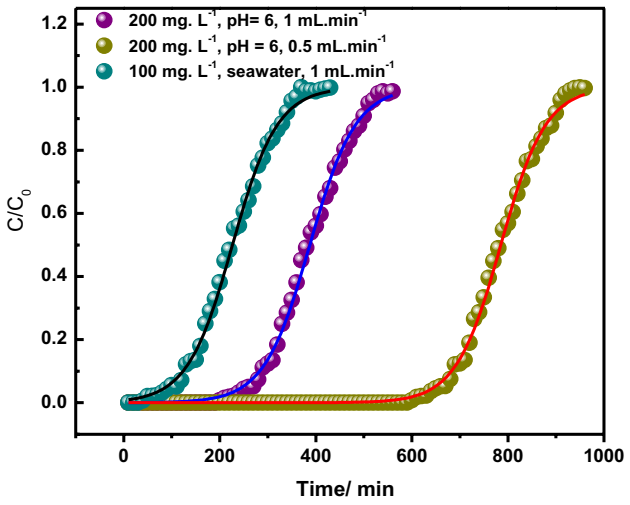

Fig. 10 Breakthrough behaviour of uranium on Si-DETA in a packed column. Adsorbent phase: Si-DETA (1 g), Aqueous phase: Uranyl nitrate solution ($U = 200$ mg L^{-1}) maintained at pH 6 or seawater spiked with uranium (100 mg L^{-1}). Flow rate of 1 mL min^{-1} and 0.5 mL min^{-1}. Temperature: 298 K

to be 77.5 and 78.5 mg g^{-1}, which are comparable with the Langmuir adsorption capacity of 78 mg g^{-1}. This indicates the efficient performance of the Si-DETA adsorbent in a packed column for the adsorption of uranium from the aqueous phase.

The performance of Si-DETA was also tested for the adsorption of uranium from seawater. The seawater was collected from the coastal area of Kalpakkam, India, and its composition is shown in Table 4 [50]. The seawater was spiked with uranium (100 mg L^{-1}), and the column study was performed. The breakthrough curve obtained for the adsorption U(VI) from seawater is shown in Fig. 10 and compared with other breakthrough curves. An early breakthrough is observed for the adsorption of uranium from seawater as compared to other cases. The breakthrough curve obtained in this case was also fitted using the Thomas model, and the fitting parameters are also shown in Table 3. The uranium adsorption capacity at 100% breakthrough was determined to be 22 mg g^{-1}. The early breakthrough and

Table 3 Fitting parameters obtained by modeling the breakthrough behavior of uranium on Si-DETA using Thomas model. Aqueous phase: 200 mg L^{-1} in pH 6 solution and 100 mg L^{-1} in seawater. Adsorbent: 1 g of Si-DETA. Temperature: 298 K

U(VI) concentration/mg L^{-1}	Flow rate/mL min^{-1}	Capacity/mg g^{-1}			K_{Th}	R^2	χ^2
		At onset	From Thomas model	From Langmuir model			
200, pH 6	1	40	77.5	78.3	0.104	0.998	2.6×10^{-4}
200, pH 6	0.5	60	78.5	–	0.107	0.998	1.7×10^{-4}
100 (sea water)	1	6	22.6	–	0.213	0.997	3.8×10^{-4}

Table 4 Elemental composition of seawater collected from costal area of Kalpakkam, India [50]

Property	Magnitude
TDS	35,600 mg L^{-1}
Suspended solids	410 mg L^{-1}
Total hardness (CaO_3)	6300 mg L^{-1}
Sodium	10,556 mg L^{-1}
Calcium	400 mg L^{-1}
Magnesium	1272 mg L^{-1}
Potassium	380 mg L^{-1}
Total alkalinity ($CaCO_3$)	138 mg L^{-1}
Chloride	18,981 mg L^{-1}
Sulfate	2650 mg L^{-1}
Fluoride	1.3 mg L^{-1}
Iron	0.1 mg L^{-1}
Silicon	0.8 mg L^{-1}
pH	8.1

lower capacity observed in the case of seawater could be due to the presence of other competing ions in seawater.

The effect of interfering ions

The effect of possible interfering ions such as CO_3^{2-}, Na^+, Cr^{+3}, Fe^{+2}, Fe^{+3}, Co^{+3}, Ni^{+3} and, VO^{2+} on the adsorption of U(VI) on Si-DETA was studied in a batch equilibration mode, and the distribution coefficient of uranium obtained in the presence of interfering ions are shown in Fig. 11. The data was compared with the distribution coefficient obtained in the absence of these elements. It can be seen that the distribution coefficient of uranium on Si-DETA in the presence of each element is reduced to some extent. The reduction is more in the presence of Fe^{+3} and Co^{2+}, perhaps due to the strong competition of these ions with uranium for adsorption on Si-DETA.

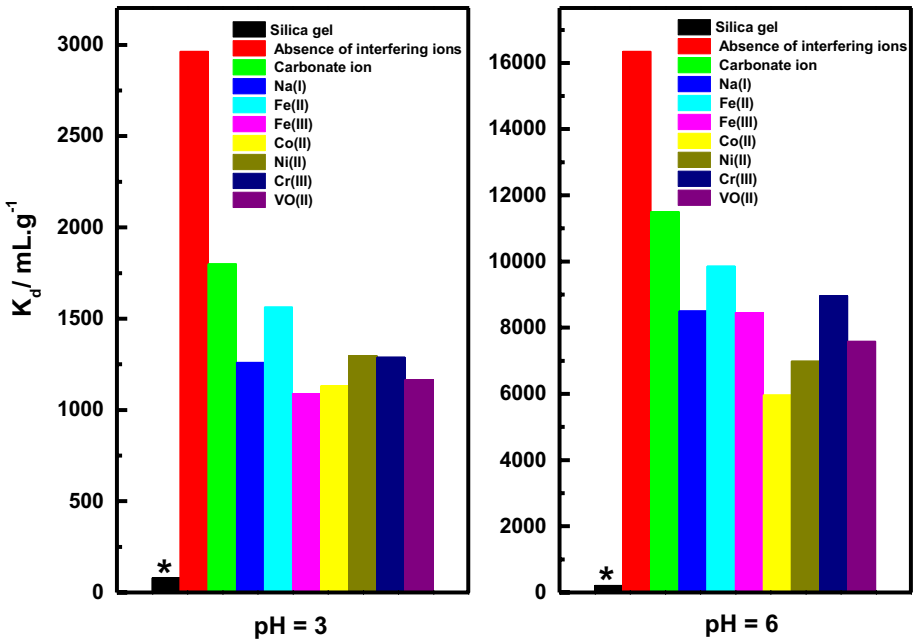

Fig. 11 Comparison in the distribution coefficient of uranium on silica gel and Si-DETA determined in the presence and absence of possible interfering ions. The * mark is for silica gel. Adsorbent: 50 mg of Si-DETA. Aqueous phase: Uranyl nitrate solution (U = 200 mg L^{-1}) and 500 mg L^{-1} of each interfering ion at pH 3 and pH 6. Temperature: 298 K

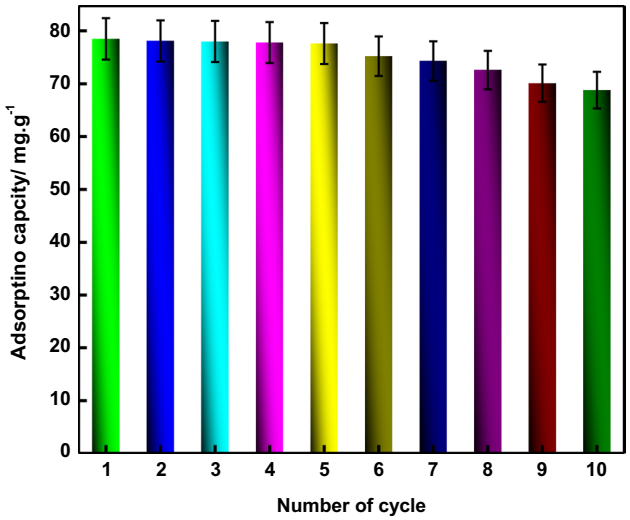

Fig. 12 Recycling behaviour of Si-DETA. Adsorbent: 50 mg of Si-DETA. Aqueous phase: Uranyl nitrate solution ($U = 2000$ mg L^{-1}) at pH 6. Temperature: 298 K

Recycling studies

Figure 12 shows the variation in the apparent adsorption capacity of uranium on Si-DETA. After loading uranium on Si-DETA, the adsorbent was separated and contacted with 0.1 M HNO_3 three times to recover uranium. After recovery, the adsorbent was washed with Millipore water and then subjected to uranium loading at pH 6. In this way, the Si-DETA was recycled 10 times. From Fig. 12, it can be seen that the adsorbent is quite efficient even after 5 times of recycling, without much loss of adsorption capacity. However, the adsorption capacity marginally decreases upon recycling more than 5 times. Around 10–15% of loss in the apparent adsorption capacity is observed upon recycling the adsorbent for ten times.

Conclusions

The Si-DETA adsorbent was prepared by anchoring of diethylenetriamine groups on silica gel by surface modification reaction. The Si-DETA was studied for the adsorption of uranium from aqueous solution as well as from seawater. The amount of DETA functional groups present on Si-DETA was determined to be 0.56 mmol per gram by thermogravimetric analysis. From FT-IR and Raman spectroscopy, the presence of an amine functional group was confirmed. The adsorption of uranium on Si-DETA was due to the coordinate bond formation between uranyl ion and amine. The morphology of all samples was not changed upon anchoring amine moieties and also upon uranium adsorption. The distribution coefficient of uranium increased with the increase of equilibrium pH, and the maximum distribution coefficient of 16,300 mL g^{-1} was obtained at pH 6 and above. The rate of adsorption of uranium on Si-DETA followed pseudo-second order rate kinetics at all concentrations of uranium and pH. The rate constant of 2.8×10^{-3} and 4.7×10^{-3} mg g^{-1} min^{-1} at the uranium concentrations of 200 and 500 mg L^{-1} in pH 6 medium was obtained. The adsorption of uranium on Si-DETA followed Langmuir type of adsorption with $K_L = 1.0 \times 10^{-2}$ mg L^{-1} and apparent adsorption capacity of 78.3 mg g^{-1} at pH 6. From the column studies, it was concluded that Si-DETA could be effectively utilized for the adsorption of uranium from aqueous solutions. The breakthrough behavior of experimental data was explained well by the Thomas model, which rendered a breakthrough capacity of 78 mg g^{-1} at 100% breakthrough for the aqueous solution spiked with uranium, and a breakthrough capacity of 22 mg g^{-1} for the seawater spiked with uranium. The adsorbed uranium was recovered quantitatively by 0.1 M HNO_3 solution and recycled about 10 times without losing much adsorption capacity. The study showed that the adsorbent Si-DETA is a potential candidate for the adsorption of uranium from both aqueous solutions as well as from seawater.

Acknowledgements The authors would like to thank Dr. S. Balakrishnan for recording TG curves. The authors also thank to Dr. Manish Chnadra for providing scanning electron microscopy facility.

References

1. Nero AV (1979) A guidebook to nuclear reactors. University of California Press
2. Jenkins JD, Zhou Z, Ponciroli R, Vilim RB, Ganda F, De Sisternes F, Botterud A (2018) The benefits of nuclear flexibility in power system operations with renewable energy. Appl Energy 15(222):872–884
3. Ingersoll DT (2009) Deliberately small reactors and the second nuclear era. Prog Nucl Energy 51(4–5):589–603
4. Shropshire D, Purvins A, Papaioannou I, Maschio I (2012) Benefits and cost implications from integrating small flexible nuclear reactors with off-shore wind farms in a virtual power plant. Energy Policy 1(46):558–573
5. Dincer I, Rosen MA (1998) A worldwide perspective on energy, environment and sustainable development. Int J Energy Res 22(15):1305–1321
6. https://www.iaea.org/newscenter/news/preliminary-nuclear-power-facts-and-figures-for-2019
7. Macfarlane AM, Miller M (2007) Nuclear energy and uranium resources. Elements 3(3):185–192
8. Azizullah M, Muhammad S, Shahzad T (2010) The importance of nuclear energy in future, major uranium deposits of the world and Pakistan. JHES 43:14–15
9. Dolchinkov NT (2019) World uranium mining production. Mach Technol Mater 13(3):127–130
10. Wang F, Liu C, Niu H, Deng Y, Ma H, Wang W (2017) Global uranium resources in sedimentary basins and the characteristics

of oil, gas, coal and uranium coexisting in one basin. Acta Geol Sin-Engl 91(s1):235–236
11. Winde F, Brugge D, Nidecker A, Ruegg U (2017) Uranium from Africa–an overview on past and current mining activities: re-appraising associated risks and chances in a global context. J Afr Earth Sci 1(129):759–778
12. Monnet A, Gabriel S, Percebois J (2017) Long-term availability of global uranium resources. Resour Policy 1(53):394–407
13. Srivastava RR, Pathak P, Perween M (2020) Environmental and health impact due to uranium mining. In: Uranium in plants and the environment 2020. Springer, Cham, pp 69–89
14. Sarkar A (2019) Nuclear power and uranium mining: current global perspectives and emerging public health risks. J Public Health Policy 40(4):383–392
15. https://www.who.int/water_sanitation_health/publications/2012/background_uranium.pdf
16. Tsouris C (2017) Uranium extraction: fuel from seawater. Nat Energy 2(4):1–3
17. Ku TL, Mathieu GG, Knauss KG (1977) Uranium in open ocean: concentration and isotopic composition. Deep-Sea Res 24(11):1005–1017
18. Zhang B, Guo X, Xie S, Liu X, Ling C, Ma H, Yu M, Li J (2016) Synergistic nanofibrous adsorbent for uranium extraction from seawater. RSC Adv 6(85):81995–82005
19. Kavaklı PA, Seko N, Tamada M, Güven O (2005) Adsorption efficiency of a new adsorbent towards uranium and vanadium ions at low concentrations. Sep Sci Technol 39(7):1631–1643
20. Zhao Y, Liu C, Feng M, Chen Z, Li S, Tian G, Wang L, Huang J, Li S (2010) Solid phase extraction of uranium(VI) onto benzoylthiourea-anchored activated carbon. J Hazard Mater 176(1–3):119–124
21. Starvin AM, Rao TP (2004) Solid phase extractive preconcentration of uranium(VI) onto diarylazobisphenol modified activated carbon. Talanta 63(2):225–232
22. Budnyak TM, Strizhak AV, Gładysz-Płaska A, Sternik D, Komarov IV, Kołodyńska D, Majdan M, Tertykh VA (2016) Silica with immobilized phosphinic acid-derivative for uranium extraction. J Hazard Mater 15(314):326–340
23. Whitty-Léveillé L, Aumaitre C, Morin JF, Reynier N, Larivière D (2019) Design of an adsorbent-bearing silica Schiff base ligand for the highly efficient removal of uranium and thorium in acidic solutions. Sep Purif Technol 228:115709
24. Ali AH, Nouh E (2019) Rhodamine-B modified silica for uranium (VI) extraction from aqueous waste samples. Sep Sci Technol 54(4):602–614
25. Al-Anber MA, Al-Momani IF, Zaitoun MA (2020) Inorganic silica gel functionalized tris(2-aminoethyl) amine moiety for capturing aqueous uranium(VI) ion. J Radioanal Nucl 325(2):605–623
26. Liu S, Luo J, Ma J, Li J, Li S, Meng L, Liu S (2021) Removal of uranium from aqueous solutions using amine-functionalized magnetic platelet large-pore SBA-15. J Nucl Sci Technol 58(1):29–39
27. Amesh P, Suneesh AS, Selvan BR, Venkatesan KA (2019) Amidic succinic acid moiety anchored silica gel for the extraction of UO_2^{2+} from aqueous medium and simulated sea water. Colloids Surf A Physicochem Eng Asp 578:123585
28. Amesh P, Suneesh AS, Venkatesan KA, Chandra M, Ravindranath NA (2020) High capacity amidic succinic acid functionalized mesoporous silica for the adsorption of uranium. Colloids Surf A Physicochem Eng Asp 602:125053
29. Amesh P, Suneesh AS, Selvan BR, Venkatesan KA, Chandra M (2020) Magnetic assisted separation of uranium(VI) from aqueous phase using diethylenetriamine modified high capacity iron oxide adsorbent. J Environ Chem Eng 8(2):103661
30. Amesh P, Venkatesan KA, Suneesh AS, Samanta N (2020) Diethylenetriamine tethered mesoporous silica for the sequestration of uranium from aqueous solution and seawater. J Environ Chem Eng 8(4):103995
31. Venkatesan KA, Sukumaran V, Antony MP, Rao PV (2004) Extraction of uranium by amine, amide and benzamide grafted covalently on silica gel. J Radioanal Nucl Chem 260(3):443–450
32. Saha B, Venkatesan KA, Natarajan R, Antony MP, Rao PV (2002) Studies on the extraction of uranium by *N*-octanoyl-*N*-phenylhydroxamic acid. Radiochim Acta 90(8):455–459
33. Khan MH, Warwick P, Evans N (2006) Spectrophotometric determination of uranium with arsenazo-III in perchloric acid. Chemosphere 63(7):1165–1169
34. Mohapatra S, Pramanik N, Mukherjee S, Ghosh SK, Pramanik P (2007) A simple synthesis of amine-derivatised superparamagnetic iron oxide nanoparticles for bioapplications. J Mater Sci 42(17):7566–7574
35. Rana S, Jonnalagadda SB (2017) Cu doped amine functionalized graphene oxide and its scope as catalyst for selective oxidation. Catal Commun 1(100):183–186
36. Corbett JF (1972) Pseudo first-order kinetics. J Chem Educ 49(10):663
37. Lagergren S (1898) Kungliga svenska vetenskapsakademiens. Handlingar 24(4):1–39
38. Ho YS, McKay G (1999) Pseudo-second order model for sorption processes. Process Biochem 34(5):451–465
39. Langmuir I (1918) The adsorption of gases on plane surfaces of glass, mica and platinum. J Am Chem Soc 40(9):1361–1403
40. Freundlich H (1926) Freundlich isotherms. Colloidal and capillary chemistry
41. Temkin MJ, Pyzhev V Recent modifications to Langmuir isotherms
42. Hutson ND, Yang RT (1997) Theoretical basis for the Dubinin–Radushkevitch (DR) adsorption isotherm equation. Adsorption 3(3):189–195
43. Reitz T, Rossberg A, Barkleit A, Steudtner R, Selenska-Pobell S, Merroun ML (2015) Spectroscopic study on uranyl carboxylate complexes formed at the surface layer of Sulfolobus acidocaldarius. Dalton Trans 44(6):2684–2692
44. Quiles F, Burneau A (1998) Infrared and Raman spectroscopic study of uranyl complexes: hydroxide and acetate derivatives in aqueous solution. Vib Spectrosc 18(1):61–75
45. Gorelik VS, Anikev AA, Korshunov VM, Voinov YP (2017) Probe Raman spectroscopy of sodium uranyl-acetate microcrystals. Opt Spectrosc 123(2):255–7
46. Thomas HC (1944) Heterogeneous ion exchange in a flowing system. J Am Chem Soc 66(10):1664–1666
47. Thomas HC (1948) Chromatography: a problem in kinetics. Ann NY Acad Sci 49(2):161–182
48. Koner S, Pal A, Adak A Use of surface modified silica gel factory waste for removal of 2, 4-D pesticide from agricultural wastewater: a case study
49. Rafati L, Ehrampoush MH, Rafati AA, Mokhtari M, Mahvi AH (2019) Fixed bed adsorption column studies and models for removal of ibuprofen from aqueous solution by strong adsorbent Nano-clay composite. J Environ Health Sci Eng 17(2):753–765
50. Hanra MS (2000) Desalination of seawater using nuclear heat. Desalination 132(1–3):263–268